Characterization of gas-water flow using electrical resistance imaging

M Wang, Y Ma, R A Williams
Institute for Particle Science and Engineering, University of Leeds, UK
Y Wu, D Li, H Li, Z Zheng
Institute of Mechanics, Chinese Academy of Sciences, P.R. China

ABSTRACT

This paper presents an impedance image based method, which is known as electrical resistance tomography (ERT), for characterization of gas-water two-phase flow in a 40m horizontal flow loop. An ERT sensor based on conductive ring technique is used to overcome the problem of measurement saturation caused by electrodes loosing electrical contact with conductive liquid, as it often occurs in stratified flow and slug or plug flow. In previous study, data implementation was constrained by the limited data collection speed and insufficient auxiliary sensing information. The quality of impedance images was also decayed due to the use of a linear back-projection algorithm. In order to gather sufficient information for the implementation of flow characteristics particularly flow pattern recognition and air cavity velocity, a fast data collection strategy was applied to a dual-plane ERT sensor and an iterative algorithm was used for image reconstruction. Results, in respect to flow patterns and velocity maps, are reported.

Keywords: ERT, gas-water two-phase flow, velocity measurement.

1 INTRODUCTION

The nature of the flow of gas-liquid mixtures in horizontal pipelines is complex, as there is a wide variety of possible flow patterns (Fig 1) which are governed principally by the physical properties (*e. g.* the density, surface tension and viscosity of the gas and liquid), the input fluxes of the two phases and the size and the orientation of the pipe. The classification proposed by Alves [1] encompasses all the major and easily recognisable flow patterns encountered in horizontal pipes. They are bubble flow, characterised by a chain of discrete gas bubble moving mainly close to the upper wall of the pipe; plug flow, bubbles interact and coalesce to give rise to large bullet shaped plugs occupying most of the pipe cross-section; stratified flow, dominated by the gravitational forces and the gas phase to flow in the upper

part of the pipe; slug flow, frothy slugs of liquid phase carrying entrained gas bubbles alternate with gas slugs surrounded by thin liquid films; annular flow, most of the liquid flowing along the inner wall of the pipe as a thin film and gas forming a central core occupying a substantial portion of the pipe cross-section; mist flow, nearly all of the liquid entrained in the gas at high gas flowrates. Since the mechanisms responsible for hold-up and momentum transfer (or frictional pressure drop) vary from one flow pattern to another, it is essential to develop some measures to predict or recognize flow patterns under specific conditions.

Also for two-phase co-current gas-liquid flow, the lack of knowledge concerning local velocities of the individual phases makes it difficult to develop any method of predicting the velocity distribution. In many instances, the gas phase may be flowing considerably faster than the liquid and continually accelerating as a result of its expansion, as the pressure falls. Either phase may be in laminar or in turbulent flow, albeit that laminar flow does not have such a clear cut meaning as in the flow of single fluids.

Three particular aspects of gas-liquid flow are of practical importance: (i) gas flow patterns or flow regimes, (ii) gas hold-up, and (iii) frictional pressure gradient.

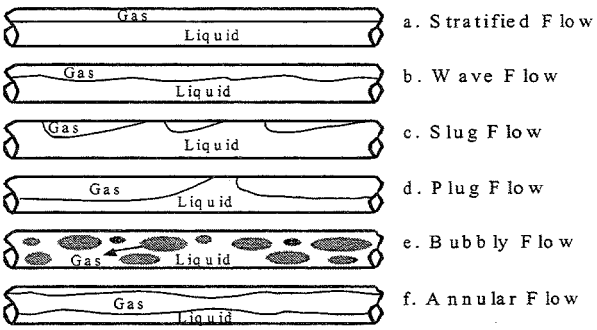

Fig 1. Gas-liquid two-phase flow patterns in a horizontal pipe

For the flow of gas-liquid mixtures, several mostly empirical attempts have been made to formulate flow pattern maps [2~7]. The regions over which the different types of the flow patterns can occur are conveniently shown as a 'flow pattern map' in which a function of the liquid flowrate is plotted against a function of the gas flowrate and boundary lines are drawn to delineate the various regions. Not only is the distinction between any two patterns poorly defined, but also the transition from one flow pattern to another may occur over a range of conditions rather than abruptly as suggested in all flow pattern maps. Furthermore, because the flow patterns are usually identified by visual observations of the flow, there is a large element of subjectivity in the assessment of the phase distribution with advanced techniques.

As to the local velocities of the individual phases, there is so far no significant methods both theoretically and experimentally to deal with them without accessing or disturbing the flow. Phase velocities are key parameters in determining flowrate or hold-up of each phase and frictional pressure gradient. Therefore, developing a tactic to measure local phase velocity is important in both theory and practice.

Electrical Resistance Tomography (ERT) developed recently for investigating flow patterns and velocity distribution of two-phase flows [9~10], is becoming increasingly promising in the study of multiphase flows because of its non-intrusive measurement and potential capacity for providing detailed information on the complex internal flow and inter-phase behaviour. In previous study, data implementation was often constrained by limited data collection speed and insufficient auxiliary sensing information. The quality of impedance images was also decayed due to the use of linear back-projection algorithm. This paper reports a much improved velocity profiles by applying a fast data collection to a dual-plane ERT sensor and an iterative image reconstruction algorithm [11]. Particular flow patterns measured with ERT are presented.

2 EXPERIMENTAL SET-UP

All the experiments described in this paper were carried out using the multiphase flow loop installed at the Institute of Mechanics, Chinese Academy of Sciences, which is a 40 meter horizontal gas-liquid flow loop with an inner diameter of 50mm. A schematic diagram or an overview of the flow loop is given in Fig 2.

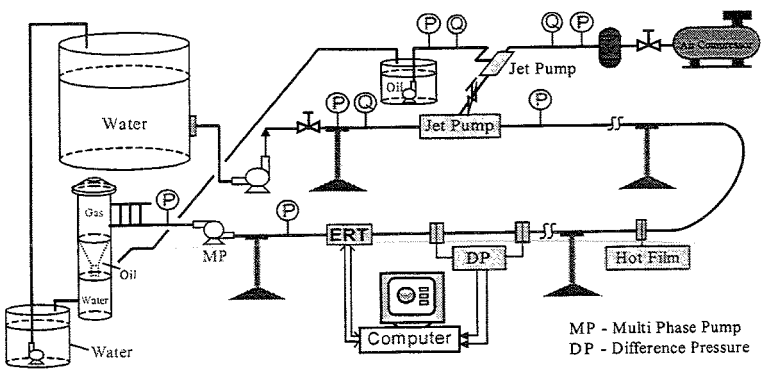

Fig 2. Schematic of the gas/water two-phase flow loop

The flow loop is fully made of transparent acrylic resin. It can run a maximum superficial liquid velocity of 1.2 m/s with Reynolds number about 40000, and a superficial gas velocity of 30 m/s with Reynolds number about 100000. The two-phases of gas and liquid, in terms of flow states of laminar to laminar, laminar to turbulent, turbulent to laminar and turbulent to turbulent, can be performed on this test-loop. By controlling the pressure and flow-rates of the gas phase and the liquid phase, many flow patterns, such as babble flow, stratified flow, plug flow, slug flow, wavy flow and annular flow, can be created in this device. The pressure, pressure difference and velocity of two-phase components are monitored using a number of pressure sensors and hot-film sensors. A tomographic sensor with three sensing planes is also installed in the flow loop in order to obtain flow patterns of particulate two-phase flow.

The tap-water (conductivity = 0.304mS/cm) was used as the liquid phase and air, introduced into the flow loop from a mixing jet-pump, as the gas phase. Measurements were performed at ambient temperature. By controlling the air flow-rate at the air inlet of the jet-pump, different flow patterns can be generated in the flow loop.

The experiments were performed under different air flow-rates of 0.5m³/h, 1.5m³/h, 4m³/h, 10m³/h and some less than 0.5m³/h in regard to the productions of bubbly flow, slug flow, slug-plug flow, and plug flow regimes. The water flows were scaled with an accumulating tank during the experiments to get water flow rate and mean velocity. At the mean time, a number of photographs were recorded as visual presentations of these different flow patterns, which were used to compare the flow patters obtained from ERT.

3 THE ERT SYSTEM

A P2000 ERT system (Industrial Tomography System Ltd., Manchester) was used for data collection. The so-called adjacent electrode pair strategy [12] was adopted, using a 15mA injection current at 9.6 kHz. Data collection rates were 50ms per frame at the signal frequency of 9.6 kHz and 16 ms per frame at the signal frequency of 38.4 kHz. Both single-plane and dual-plane ERT sensors were used in this study. Each ERT sensing plane consisted of 16 titanium-alloy rectangular electrodes (5mm×12mm). A conductive ring technique was applied to overcome the problem of measurement saturation caused by electrodes loosing electrical contact with conductive liquid, as it often occurs in stratified flow and slug flow [13]. The dual-plane ERT sensor was a core in the experiment for the implementation of local flow velocities in the two-phase flow.

Since the data collection speed from the system was still limited, we set the distance between the two sensing planes apart further to 590mm. According to the results from visual observation and tomographic imaging, the shapes and sizes of flow patterns at the downstream of the flow loop were quite stable, which were also proved by the movies taken in this experiment. To improve the correlation, a dual-plane measurement strategy was applied, which had been built into the ITS P2000 ERT system. The principle of the dual-plane strategy is based on a 'cross measurement between two correlated electrodes on two sensing planes' instead of that the measurement was carried plane by plane. However, the dual-plane strategy may be not suitable for flow pattern reconstruction due to its low data collection speed (always on two planes) and relevant poor signal-to-noise-ratio. In order to reduce the error caused by the point-spread function in the used of the SBP algorithm, an iterative algorithm, known as SCG algorithm [11], was utilized to solve the non-linear problem of the electric field. All images used for implementation of local velocities in the paper were reconstructed with the SCG. The measurements for flow pattern recognition were performed by the use of one sensing plane only in order to get maximum data acquisition speed.

The dimension of the sensing planes installation is given in Fig 3, and a photograph of the set-up is shown in Fig 4.

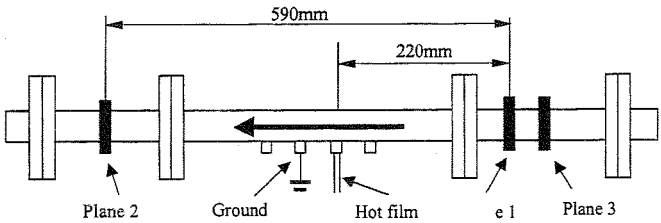

Fig 3. Sensor configuration

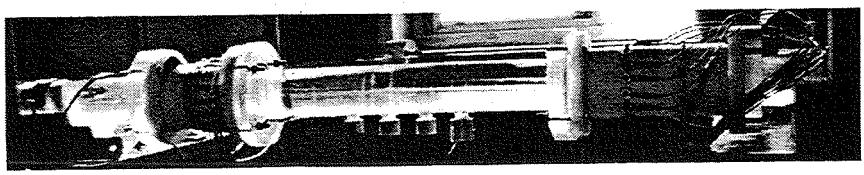

Fig 4. The photograph of the sensor

4 EXPERIMENT RESULTS

4.1 Flow pattern recognition

Bubbly flow at superficial velocities of air 0.00354 m/s, water 0.609 m/s (620 frames, taken in 10 seconds)

Bubbly flow at superficial velocities of air 0.0071 m/s, water 0.605 m/s (620 frames, taken in 10 seconds)

Bubbly flow at superficial velocities of air 0.01415 m/s, water 0.605 m/s (620 frames, taken in 10 seconds)

Short slug flow at superficial velocities of air 0.03536 m/s, water 0.59 m/s (620 frames, taken in 10 seconds)

Long slug flow at superficial velocities of air 0.0707 m/s, water 0.538 m/s (620 frames, taken in 10 seconds)

Plug flow at superficial velocities of air 0.2122 m/s, water 0.563 m/s (620 frames, taken in 10 seconds)

Plug flow at superficial velocities of air 0.566, water 0.515 m/s (620 frames, taken in 10 seconds, threshold value 0.0-0.2)

Plug flow at superficial velocities of air 1.4145 m/s, water 0.484 m/s (620 frames, taken in 10 seconds, threshold value 0.0-0.2)

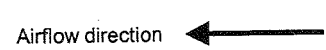

Fig 5. Flow patterns *vs* different air flowrates (black denotes air phase and grey denotes water phase, images were reconstructed using SBP)

Flow pattern recognition was obtained with data from the single-plane ERT sensor (plane 3 in Fig 3). In order to obtain better time-resolution, the data collection speed was set as 62 frames/sec. Images were reconstructed using SBP (sensitivity coefficient back-projection) algorithm. Stacking part of the reconstructed tomograms, the gas-phase and liquid-phase distribution and the dynamically varying processes (flow processes) in the pipe can be clearly visualised. Flow patterns varied with air flowrates are illustrated in Fig 5, which were resulted from ERT reconstruction.

4.2 Flow velocity measurement

Applying cross-correlation technique to extract the speed of moving profiles had been widely demonstrated [14]. Depending on the sensing strategies, whether the data coming from one sensing plane or two sensing planes, the implementation of 'features' velocity can be based on either the auto-correlation method [8] or the cross-correlation method [15]. The basic concept of correlation is to find the transition time between two profiles obtained between the two sections acquired from one sensing plane or from a dual-plane sensor. With a mathematical description, it intends to find a transition time τ that can make the difference, ε, minimum. This can be achieved by using the least square criterion as given by the following equation: To investigate gas phase velocity in the air/water two-phase flow, data were collected from the duel-plane sensor at different gas flow rates. Cross-correlation method was used to implement the gas velocity.

$$\varepsilon^2{}_{xy}(\tau) = \min \lim_{T\to\infty} \frac{1}{T} \int_{-T}^{T} \left[x(t) - y(t-\tau)\right]^2 dt \qquad (1)$$

where x, y are the original signals of void fraction at each imaging cross section respectively, ε is the error function which gives the transition time τ when the expression take a minimum value. Replacing the integral by partial summation, equation (1) can be expressed in discrete form:

$$\varepsilon_k^2(n) = \sum_{m=0}^{M-n} \left[x_k(m) - y_k(m-n)\right]^2 \qquad (2)$$

where M is sample length, n is correlated sample ($n = 1, \cdots, M-1$) and k is the number to indicate different pixels on the cross-section.

In the computation, M should be selected according to the distance between the dual-plane ERT sensors and the maximum and the minimum velocity of the flow. M is selected amongst 100~700 (images) in this study.

It should be noted that equation (1) could be deduced to the following form:

$$\begin{aligned} \varepsilon^2{}_{xy}(\tau) &= \min \lim_{T\to\infty} \frac{1}{T} \int_{-T}^{T} \left[x(t) - y(t-\tau)\right]^2 dt \\ &= \min \lim_{T\to\infty} \frac{1}{T} \int_{-T}^{T} \left[x(t)^2 + y(t-\tau)^2 - 2x(t)y(t-\tau)\right] dt \end{aligned} \qquad (3)$$

To take the minimum value of equation (3), it can be expressed as:

$$R = \max \lim_{T \to \infty} \int_{-T}^{T} x(t) \cdot y(t-\tau) dt \qquad (4)$$

or, in a discrete form of a partial summation:

$$R_k(n) = \sum_{m=0}^{M-n} x_k(m) \cdot y_k(m-n) \qquad (5)$$

Equation (4) and (5) were recognised as short forms of equation (1) and (2) and were used in some of previous researches [8, 16]. However, we found this may cause relatively larger errors on the results because only a finite integral range can be applied in the practice, other than an infinite integral range in equation (3). It is not always true that in a practical correlation range, the integral of $y(t-\tau)^2$ over a practical correlation range is an unchanged constant. Therefore, we propose directly applying equation (1) and its discrete form (2) to carry out cross-correlation when needed as we did in this paper.

Correlations between some stacked images, as given in Figure 6 in respond to three air flowrates (25 L/H, 500 L/H and 4000 L/H), are reviewed. The correlations are obviously, which demonstrates the dual-plane mode at the data collection speed of 31.3 dual-frames/second is able to manage the velocities at the demonstrated mean air flowrates.

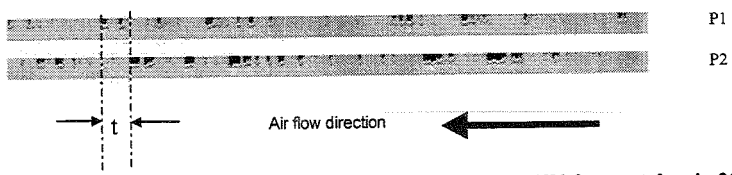

(a) Bubbly flow at superficial velocities of air 0.00354m/s, water 0.628 m/s (620 frames, taken in 20 seconds)

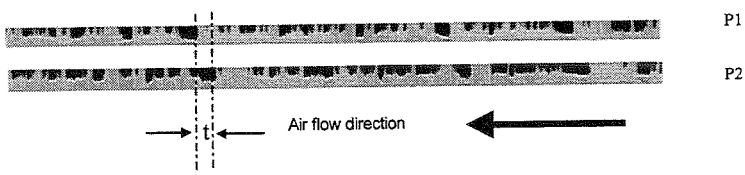

(b) Slug flow at superficial velocities of air 0.0707 m/s, water 0.59 m/s (620 frames, taken in 20 seconds)

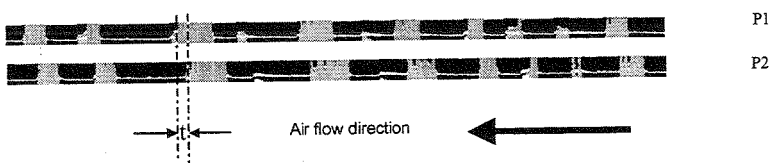

(c) Plug flow at superficial velocities of air 0.566 m/s, water 0.528 m/s (620 frames, taken in 20seconds, threshold value 0.0-0.2)

Fig 6. Cross-correlation between two images obtained from dual-plane ERT sensor.

The gas-phase velocity converted from the cross-correlation results can be calculated by:

$$v = \frac{\Delta s}{\Delta t} = \frac{0.59}{(n_k - 1)/31.3} \tag{7}$$

where n_k is the correlated sampling length (or sampling number to result a minimum value from equation (1) or (2).

Applying the cross-correlation procedure to a data set of 2000 frame of tomographic images, that were acquired from the air/water two-phase horizontal pipe flow and reconstructed using the SCG algorithm, velocity distributions of the two-phase flow were obtained, which are given in Fig 7. Evidences of the correlation at each pixel can be confirmed from viewing of its correlation curve, and as well comparing their flow pattern. Typical correlation curves are provided in Fig 7, in respect to their relevant flow conditions. Fig 7 shows the velocity distribution, resulted from the cross-correlation implementation, for a bubbly flow, a slug flow and a plug flow. The average velocities of the gas phase (patterns) implemented from the cross-correlation are approximated as about 0.622, 0.863 and 1.383 m/s (the threshold values used for identifying the interface between the water and gas are 0.7, 1.0 and 1.5 m/s, respectively), in respect to the water phase velocities of 0.798, 1.058 and 1.591 m/s (see discussion in next section). The superficial velocities estimated in the experiments are 0.628 m/s, 0.590 m/s and 0.528 m/s for water and 0.004 m/s, 0.071 m/s and 0.5662 m/s.

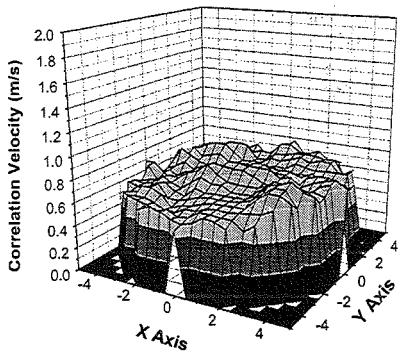

(a) bubbly flow (v_w=0.628 m/s, v_a=0.004 m/s)

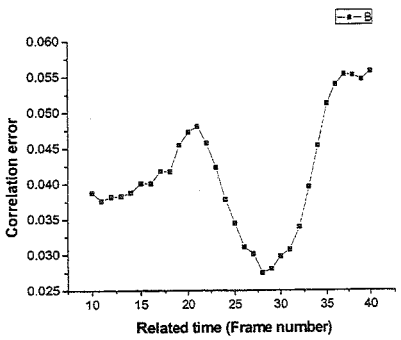

(b) a typical correlation error

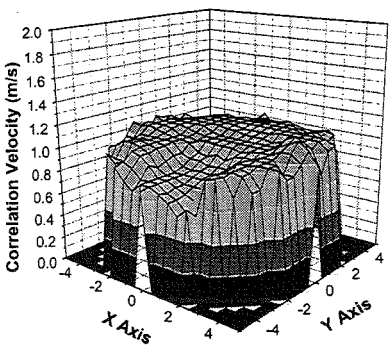

(c) slug flow (v_w=0.59 m/s, v_a=0.071 m/s)

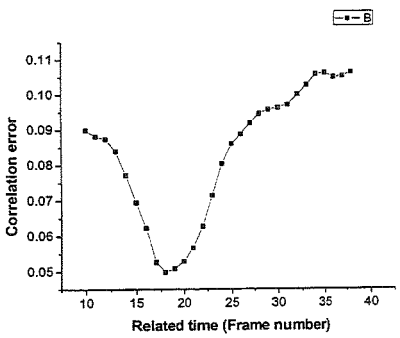

(d) a typical correlation error

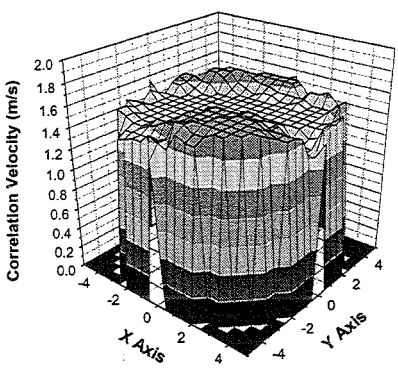

(e) plug flow (v_w=0.628 m/s, v_a=0.567 m/s)

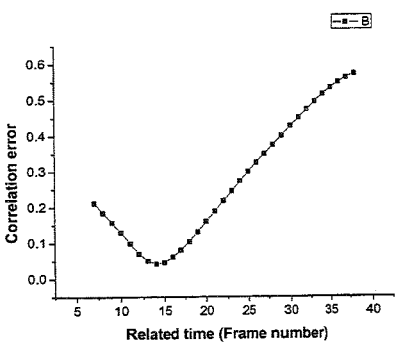

(f) typical correlation errors

Fig 7. Phase-velocity distributions *vs* different flow patterns, where v_w denotes the estimated superficial velocity of the water; v_a denotes the estimated superficial velocity of the air. The point at x=0, y=-5 in the coordinate of these images is in respect to the top of the cross-section of the horizontal pipeline).

5 DISCUSSIONS AND CONCLUSIONS

From the main results of Fig (5), (6) and (7) in this paper, useful information and interesting phenomena, on both the gas-liquid two-phase flow and ERT technique, can be found. Firstly, the results proves the electrical resistance tomography technique with a conducting ring sensing technique is a suitable means in detecting the flow patterns of gas-liquid multiphase flow. With a fast data collecting strategy and an effective image reconstruction algorithm, gas-phase and liquid-phase distribution and their dynamically varying processes (flow processes) in the pipe can be visualised (Fig 5). Secondly, the magnitude of the velocity distribution in both the gas-phase and liquid-phase can be implemented from tomographic concentration images. The cross-correlation time of the bubbly flow is observed to be longer than that of the slug flow, and much longer than that of the plug flow (Fig 6), which is also proved from velocity maps (Fig 7) by applying cross-correlation.

The degree of the cross-correlation of the flow increases with the increase of gas flowrate (see Fig 6). This comment is also supported by the facts that, in slug or plug flow, the cross-correlation graphics can be obtained almost on every pixel in Fig 7c, but only on partial pixels in bubbly flow in Fig 7a. It was unexpected that strong correlations can be found in the water phase (see the two flat parts of Fig 7c). Due to the apparent difference between the two mean velocities of the water and gas phases, the correlation results are unlikely manipulated from the possible errors introduced in image reconstruction, such as the artificial noises and the effect of linear interpolation. Therefore, the reason for the correlation in water phase may be suggested as clusters of fine gas bubbles were mixed in the water, and then ERT reported such concentration distribution in their images. Although the tendency of the increase of flow rates of both phases due to the increase of gas flow rate is obviously right, significant tolerances exist between the measured and estimated values. For an example, for a flow with superficial velocities of 0.590 m/s and 0.071 m/s in respect to water and gas (see Fig 7c), the high velocities of the water phases up to 1.058 m/s are suspected. Validation of the results with other auxiliary sensors will be performed and results will be reported in future.

Acknowledgments

The authors gratefully acknowledge the supports of Royal Society-Chinese Academy of Sciences (under Joint Project: Q783), and CAS & CNOOC (under grant KJCX2-SW-L03).

REFERENCES

[1] Alves, G E (1954) *Chem. Eng. Prog.* **50** 449.

[2] Hewitt, G F (1978) *Measurement of two-phase flow parameters*. Academic, New York.

[3] Hewitt, G F (1982) in *Handbook of Multiphase systems*. edited by Hetsroni, G., McGraw Hill, New York, pp. 2-52.

[4] Govier, G W and Aziz, K (1982) *The flow of complex mixtures in pipes*. Krieger, R E Malabar, F L.

[5] Hetsroni, G (Ed.) (1982) *Handbook of Multiphase systems*, McGraw Hill, New York.

[6] Chisholm, D (1983) *Two phase flow in pipelines and heat exchangers*. George Goodwin London.

[7] Ferguson, M E G and Spedding, P L (1995) *J. Chem. Tech. Biotech.* **62** 262.
[8] Wang, M and Yin, W (2001) *Tras IChemE*, **79**, Part A, pp. 883-886.
[9] Wang, M, Dorward, A, Vlaev, D & Mann, R (2000) *Chem. Eng. J.* 77, pp. 93-98.
[10] Mann, R, Wang, M, Forrest, A E, Holden, P J, Dickin, F J, Dyakowski, T, & Edwards, R B (1999) *Chem. Eng. Comm.* **175**, pp. 39-48.
[11] Wang, M (2002) *Measurement Science and Technology*, **13**, pp101-117.
[12] Brown, B H, and Segar, A D, (1985) Applied potential tomography: Data collection problems, *Proc IEE Int Conf on Electric and Magnetic Field in Medic and Biolo*, pp. 79-82.
[13] Wang M and Yin W (2002) *Measurement Science and Technology*, **13**, pp. 1884-1889.
[14] Beck, M S and Plaskoeski, A (1987) *Adam Hilger*, Bristol, UK.
[15] Lucas, G P, Cory, I, waterfall, R, Loh, W W and Dickin, F J (1999) *Journal of Flow Measurement and Instrumentation*, **10**(4), pp.249-258
[16] Loh, W W, Waterfall, R C, Cory, J and Lucas, G P (1999) *Proc of 1st World Congress on Industrial Tomography*, Buxton, UK, pp. 47-53.